Supporting Information

Green and Size-Specific Synthesis of Stable Fe-Cu Oxides as Earth-Abundant Adsorbents for Malachite Green Removal

Ping Zhang [1], Deyi Hou [1,*], Xuanru Li [1], Simo Pehkonen [2], Rajender S. Varma [3], Xun Wang [4],

[1] School of Environment, Tsinghua University, Beijing 100084, China

[2] Department of Environmental and Biosciences, University of Eastern Finland, Kuopio 70211, Finland

[3] Water Resources Recovery Branch, Water Systems Division, National Risk Management Research Laboratory, US Environmental Protection Agency, Cincinnati, Ohio 45268, USA.

[4] Department of Chemistry, Tsinghua University, Beijing 100084, China

*Corresponding author: Email: houdeyi@tsinghua.edu.cn

Number of pages: 10

Number of Figures: 7

Number of Tables: 3

Adsorption kinetics studies

To understand the essence of the adsorption process, the pseudo-first-order kinetics model, pseudo-second-order kinetics model, and intraparticle diffusion model were adopted to analyse the adsorption kinetics [1-2]. These models can be expressed as follows:

$$\ln(q_e - q_t) = \ln q_e - k_1 t \quad \text{(S1)}$$

$$t/q_t = 1/(k_2 q_e^2) + t/q_e \quad \text{(S2)}$$

$$q_t = k_{pi} t^{1/2} + C_i \quad \text{(S3)}$$

where q_e and q_t (mg/g) are the amounts of MG dye adsorbed at equilibrium and given time, respectively. k_1 (min^{-1}), k_2 (g/mg/min) and k_{pi} (mg g^{-1} $min^{-0.5}$) represent the rate constants of pseudo-first-order, pseudo-second-order, and intraparticle diffusion model, respectively. C_i is a constant (mol/g), which can be used to determine whether the controlling step is intraparticle diffusion [3]. If the q_t is linear with $t^{1/2}$ and the value of C_i is zero, the adsorption process is controlled by the intraparticle diffusion only; if the results of curve fitting contain multi-line plots, then there exists two or more steps in the adsorption process [3].

Adsorption thermal studies

To better illustrate the adsorption behaviour between the adsorbate and the adsorbent in the solution, the Langmuir, Freundlich, and Dubinin-Radushkevish (D-R) isotherm models were used to describe the adsorption processes[4]. The Langmuir isotherm model is based on the hypothetical premise that monolayer adsorption occurs at the specific homogeneous sites within the adsorbent [5]. The Freundlich adsorption isotherm model is founded on the assumption that the interactive behavior is related to multiple-layer adsorption occurring on the heterogeneous surface with different adsorption energies and affinities [5]. The

Dubinin-Radushkevish (D-R) isotherm model is usually adopted to distinguish whether the adsorption is physical or chemical [6]. The three model equations can be described as follows:

$$C_e/q_e = 1/(q_m K_L) + C_e/q_m \quad \text{(S4)}$$

$$\ln q_e = \ln K_F + \frac{1}{n}\ln C_e \quad \text{(S5)}$$

$$\ln q_e = ln q_m - k\varepsilon^2 \quad \text{(S6)}$$

where C_e is the equilibrium concentration of MG (mg L^{-1}), q_e is the quantity of MG adsorbed per gram of sample after equilibrium (mg g^{-1}), q_m represents the maximum adsorption capacity (mg g^{-1}), K_L is the Langmuir adsorption constant (L mg^{-1}), K_F and 1/n are the proper constants of the Freundlich isotherm, which are respectively represented by the adsorption capacity and adsorption intensity [5]. Finally, k ($mol^2 \cdot kJ^{-2}$) is the D-R isotherm constant ($E = \frac{1}{\sqrt{2k}}$, when E < 8 kJ mol^{-1}, it is physisorption and if it is between 8-16 kJ mol^{-1}, it is chemical in nature), and ε represents Polanyi potential ($\varepsilon = RT\ln(1+1/C_e)$).

The Langmuir isotherm is also expressed in terms of a dimensionless constant called a separation factor (R_L), which is defined by Eq. S7:

$$R_L = 1/(1 + K_L C_0) \quad \text{(S7)}$$

where C_0 (mg L^{-1}) is the initial MG concentration. The R_L value indicates the isotherm is favourable ($0 < R_L < 1$), unfavourable ($R_L > 1$), linear ($R_L = 1$), or irreversible ($R_L = 0$) [7].

Adsorption thermodynamic studies

Thermodynamic parameters, such as the Gibbs free energy (ΔG), the enthalpy changes (ΔH), and the entropy change (ΔS), can provide further information. The values of ΔG, ΔH and ΔS can be obtained by the following equations:

$$K_d = \frac{q_e}{C_e} \quad \text{(S8)}$$

$$\Delta G_0 = \Delta H_0 - \mathrm{T}\Delta S_0 \qquad \text{(S9)}$$

$$\ln K_d = -\Delta H_0/(RT) + \Delta S_0/R \qquad \text{(S10)}$$

where K_d is the equilibrium constant (mL/g), q_e is the adsorption capacity (mg/g), and C_e is the MG concentration at equilibrium(mg/L). R is the universal gas constant (8.314 J /(mol·K)) and T is the absolute temperature (K). The thermodynamic parameters ΔH and ΔS can be obtained from the slope and the intercept of the linear plot of ln K_d vs. 1/T.

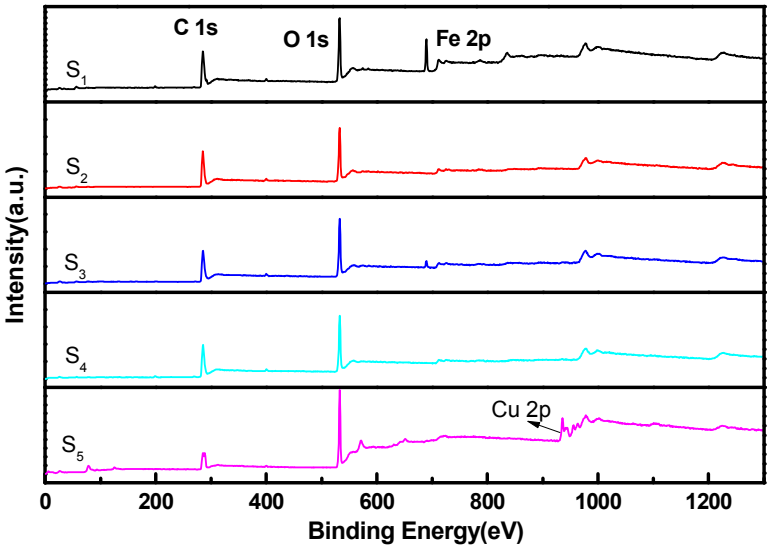

Fig S1. XPS survey spectra of S_1-S_5 samples.

As displayed in Fig S1, the peaks of the XPS full spectra indicated that C, O, and Fe were the predominant elements in S_1-S_5 samples. The peak for the copper element was not obvious in the S_1-S_4 samples due to its low content or its high dispersibility.

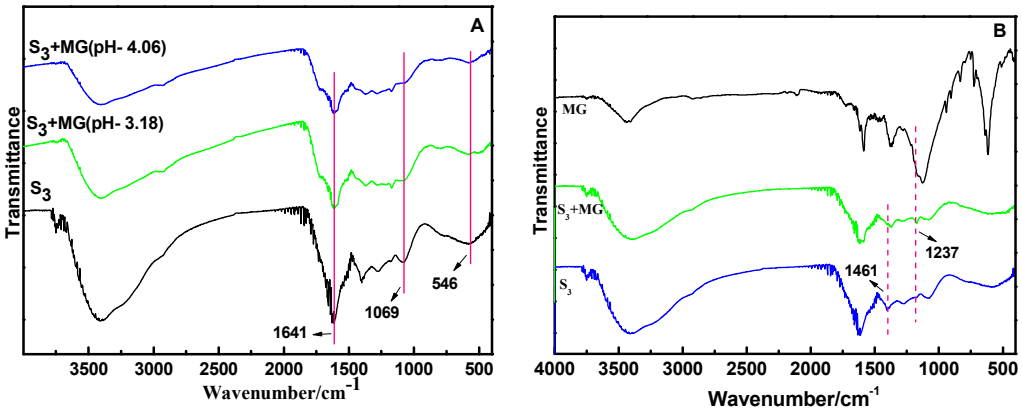

Fig S2. FTIR spectra of (A) S_3, and S_3 after MG adsorption (S_3+MG) in low initial pH solutions (pH 4.06 and pH 3.18), and (B) S_3, MG and S_3 after adsorption (S_3+MG).

As shown in Fig S2A, the FTIR spectra of S_3 after adsorption at low initial pH values were compared with the spectrum of S_3 before adsorption. The spectrum showed similar adsorption peaks before and after adsorption (1641cm^{-1} for C=C aromatic ring stretching vibration, 1069 cm^{-1} for C=O of carboxylic acid, 546 cm^{-1} refer to metal-oxygen stretch in metal oxides, etc.).

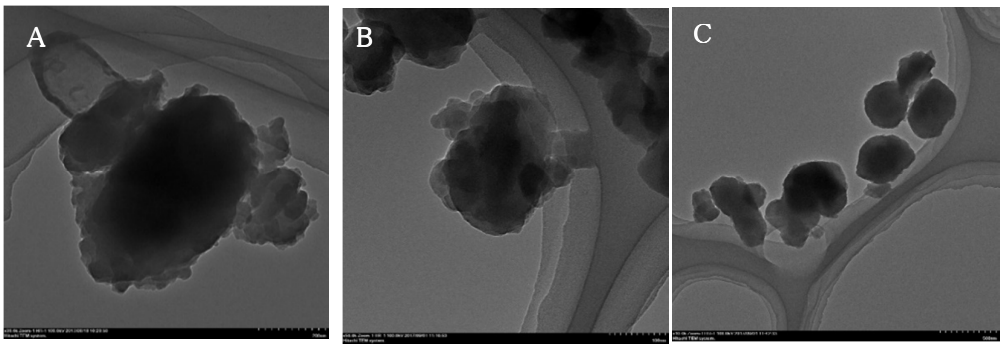

Fig S3. TEM images of (A) S_1, (B) S_2, and (C) S_4

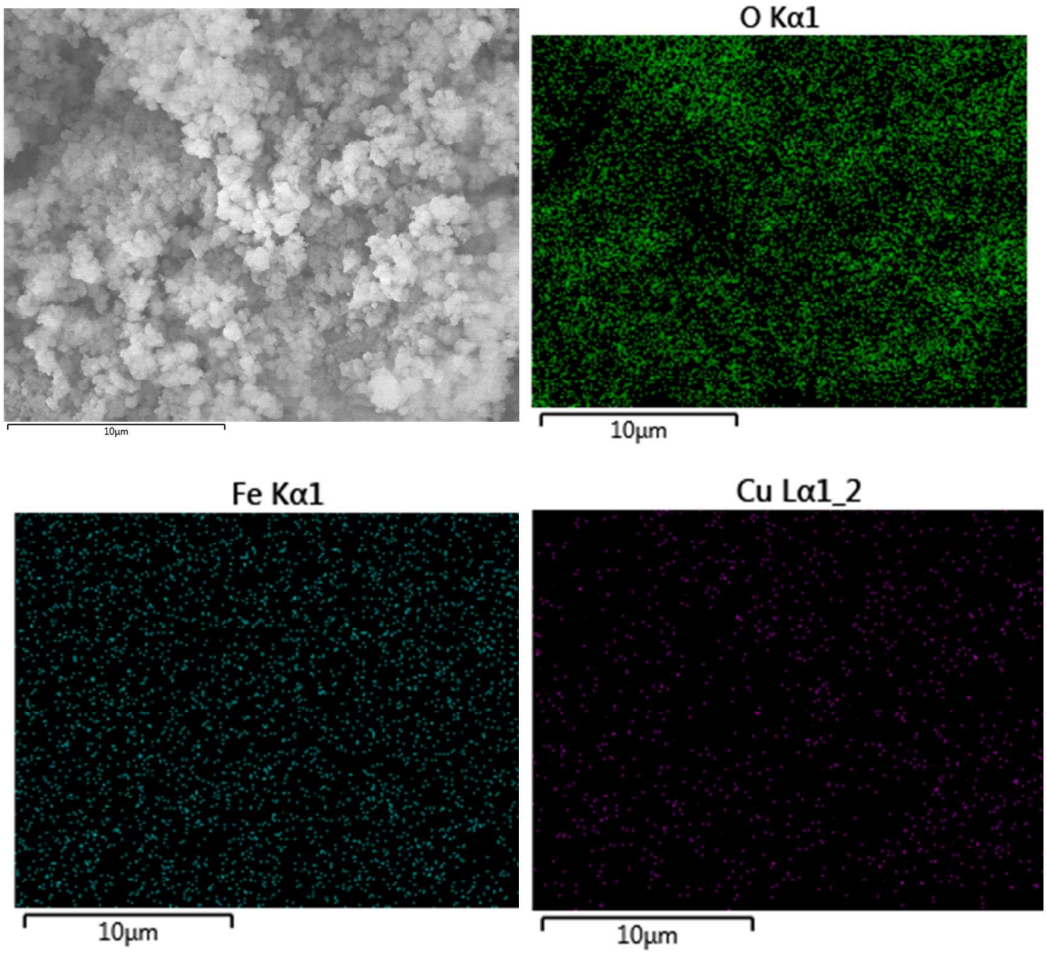

Fig S4. SEM images of the S_3 sample and the corresponding elemental (O, Fe, Cu) mapping.

The SEM image of S_3 sample and its corresponding elemental mapping are shown in Figure S4; green, blue and red images indicate the O-, Fe- and Cu-enriched areas of the sample, which implied that the elements are well dispersed on the surface of the S_3 sample.

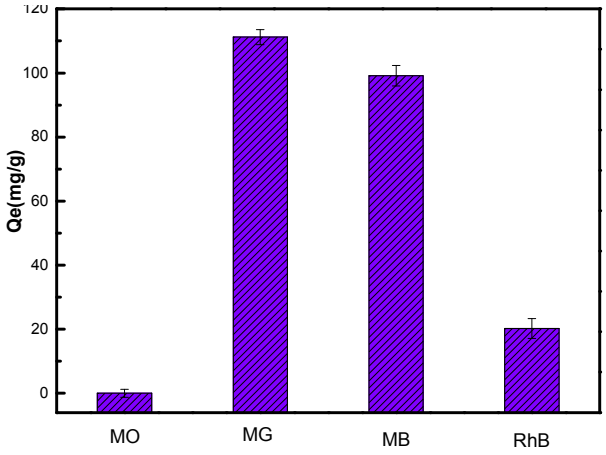

Fig S5. The adsorption capacity of S_1 sample for MO, MG, MB, RhB dyes (dosage = 0.3g/L; C_0: 50mg/L, T = 303 K, unadjusted pH).

Different dyes (MO, MG, MB, RhB) were used to test the adsorption capacity of S_1 sample. As seen from Fig S5, the removal efficiency for MG was greater than MO, MB and RhB, therefore MG dye was selected as the research object.

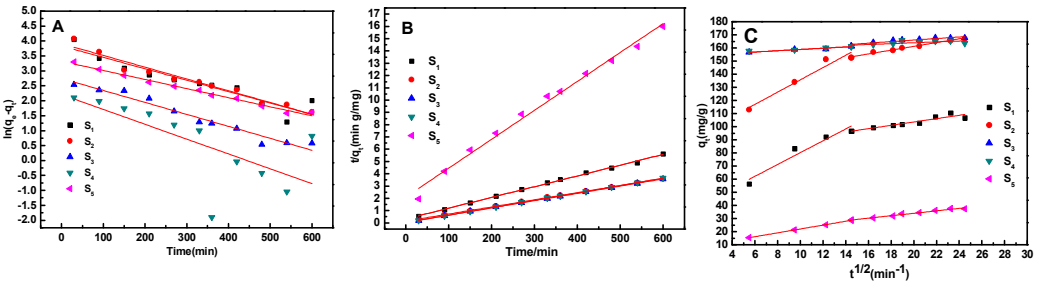

Fig S6. Kinetics of MG removal by S_1-S_5 samples, modelled by (A) Pseudo-first-order, (B) Pseudo-second-order, and (C) Intraparticle diffusion model (unadjusted pH = ~6.6; T = 303 K ; dosage = 0.006 g/20 mL).

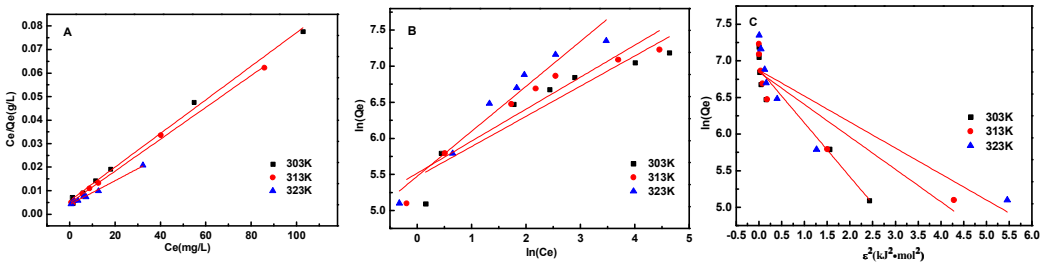

Fig S7. MG adsorption by S_3 at different temperatures modelled by (A) Langmuir model (B) Freundlich model, and (C) D-R model (unadjusted pH = ~6.6; T = 303-323 K; dosage = 0.006 g/20 mL; C_0 = 50–500 mg/L)

Table S1 Kinetic parameters of models for different samples.

	Langmuir isotherm				Freundlich isotherm			D-R isotherm		
T	Q_{max}	K_L	R_L	R^2	K_F	n	R^2	Q_{max}	E	R^2
(K)	(mg g^{-1})	(L mg^{-1})			(L g^{-1})			(mg g^{-1})	(kJ mol^{-1})	
303	1399	0.125	0.016-0.138	0.996	237	2.389	0.857	980	1.166	0.914
313	1476	0.143	0.014-0.123	0.998	249	2.254	0.893	942	1.502	0.834
323	1977	0.123	0.016-0.139	0.990	238	1.603	0.935	967	1.679	0.738

Table S2. Isotherm constants and values of R^2 for S_3 sample.

T(K)	Langmuir isotherm			Freundlich isotherm			D-R isotherm		
	Q_m(mg /g)	K_L (L/mg)	R^2	K_F (L/g)	n	R^2	Q_m(mg/g)	E(kJ/mol)	R^2
303	1399	0.125	0.996	237	2.389	0.857	980	1.166	0.914
313	1476	0.143	0.998	249	2.254	0.893	942	1.502	0.834
323	1977	0.123	0.990	238	1.603	0.935	967	1.679	0.738

Table S3. Thermodynamics parameters for MG adsorption on the S_3 sample.

Temperature (K)	ΔG^0 (kJ mol $^{-1}$)	ΔH^0 (kJ mol $^{-1}$)	ΔS^0 (J mol $^{-1}$K $^{-1}$)
303	-10.647		
313	-11.837	25.398	118.96
323	-13.026		

References

1. Lu, Y.; Zhu, H.; Wang, W.-J.; Li, B.-G.; Zhu, S., Collectable and Recyclable Mussel-Inspired Poly(ionic liquid)-Based Sorbents for Ultrafast Water Treatment. *ACS Sustainable Chemistry & Engineering* **2017,** *5* (4), 2829-2835.
2. Luo, X.; Liu, C.; Yuan, J.; Zhu, X.; Liu, S., Interfacial Solid-Phase Chemical Modification with Mannich Reaction and Fe(III) Chelation for Designing Lignin-Based Spherical Nanoparticle Adsorbents for Highly Efficient Removal of Low Concentration Phosphate from Water. *ACS Sustainable Chemistry & Engineering* **2017,** *5* (8), 6539-6547.
3. Yu, M.; Han, Y.; Li, J.; Wang, L., CO 2 -activated porous carbon derived from cattail biomass for removal of malachite green dye and application as supercapacitors. *Chemical Engineering Journal* **2017,** *317*, 493-502.
4. Rajak, R.; Saraf, M.; Mohammad, A.; Mobin, S. M., Design and construction of a ferrocene based inclined polycatenated Co-MOF for supercapacitor and dye adsorption applications. *J. Mater. Chem. A* **2017,** *5* (34), 17998-18011.
5. Zou, Y.; Liu, Y.; Wang, X.; Sheng, G.; Wang, S.; Ai, Y.; Ji, Y.; Liu, Y.; Hayat, T.; Wang, X., Glycerol-Modified Binary Layered Double Hydroxide Nanocomposites for Uranium Immobilization via Extended X-ray Absorption Fine Structure Technique and Density

Functional Theory Calculation. *ACS Sustainable Chemistry & Engineering* **2017,** *5* (4), 3583-3595.
6. He, S.; Zhang, F.; Cheng, S.; Wang, W., Synthesis of Sodium Acrylate and Acrylamide Copolymer/GO Hydrogels and Their Effective Adsorption for Pb2+and Cd2+. *ACS Sustainable Chemistry & Engineering* **2016,** *4* (7), 3948-3959.
7. Hu, J.; Deng, W.; Chen, D., Ceria Hollow Spheres As an Adsorbent for Efficient Removal of Acid Dye. *ACS Sustainable Chemistry & Engineering* **2017,** *5* (4), 3570-3582.